3

Statistical Mechanics of Quantum Plasmas. Path Integral Formalism.

A. ALASTUEY

Laboratoire de Physique. Ecole Normale Supérieure de Lyon, 69364 Lyon Cedex 07. France

Abstract

In this review, we consider a quantum Coulomb fluid made of charged point particles (typically electrons and nuclei). We describe various formalisms which start from the first principles of statistical mechanics. These methods allow systematic calculations of the equilibrium quantities in some particular limits. The effective-potential method is evocated first, as well as its application to the derivation of low-density expansions. We also sketch the basic outlines of the standard many-body perturbation theory. This approach is well suited for calculating expansions at high density (for Fermions) or at high temperature. Eventually, we present the Feynman-Kac path integral representation which leads to the introduction of an auxiliary classical system made of extended objects, i.e., filaments (also called "polymers"). The familiar Abe-Meeron diagrammatic series are then generalized in the framework of this representation. The truncations of the corresponding virial-like expansions provide equations of state which are asymptotically exact in the low-density limit at fixed temperature. The usefulness of such equations for describing the inner regions of the sun is briefly illustrated.

Abstract

Dans cette revue, nous considérons un fluide coulombien quantique con-

https://doi.org/10.1017/S0252921100026312 Published online by Cambridge University Press

stitué de charges ponctuelles (typiquement des électrons et des noyaux). Nous décrivons différents formalismes s'appuyant sur les premiers principes de la mécanique statistique. Ces méthodes permettent de calculer les quantités d'équilibre de manière systématique dans des limites particulières. La méthode des potentiels effectifs est d'abord évoquée, ainsi que son application aux développements à basse densité. Nous résumons aussi les grandes lignes de la théorie de la perturbation à N corps. Cette approche est bien adaptée au calcul des développements à haute densité (pour des fermions) ou bien à haute température. Finalement, nous exposons la représentation de Feynman-Kac qui conduit à l'introduction d'un système classique auxiliaire constitué d'objets étendus, i.e., les filaments (aussi appelés "polymères"). Les séries diagrammatiques de Abe et Meeron habituelles sont alors généralisées dans le cadre de cette représentation. Les développements correspondants de type viriel, fournissent des équations d'état qui deviennent asymptotiquement exactes dans la limite de basse densité à température donnée. L'utilité de telles équations pour décrire les régions internes du soleil est brièvement illustrée.

3.1 Introduction

In many situations, dense stellar matter can be described in terms of quantum plasmas made of electrons and nuclei. Beside its own conceptual interest, the study of the equilibrium properties of such systems turns then to be quite useful for astrophysics. Here, we review first principle formalisms with main emphasis on the path integral representation.

First, we define the model and we recall the theorems which guarantee its thermodynamics stability. In Section 2, we describe few standard methods. In section 3, we present the Feynman-Kac representation which leads to the introduction of an equivalent system made of filaments (also called "polymers" in the literature). The corresponding formalism is applied to the derivation of low-density expansions of the thermodynamic functions in Section 4. It is shown that these expansions can be systematically inferred from diagrammatic series where the usual long-range Coulomb divergencies are resummed by a technique similar to what Meeron (1958) and Abe (1959) did in the purely classical case. As exposed in Section 5, the truncations of the expansion of the pressure provide analytic equations of state (EOS) which should be rather accurate at relatively low densities and high temperatures. For instance, these conditions are met in the core of the Sun which can be viewed, as a first approximation, as a three-component plasma made of electrons, protons and Helium nuclei.

https://doi.org/10.1017/S0252921100026312 Published online by Cambridge University Press

This review is mostly dedicated to a qualitative description of the basic mechanisms and identities underlying the formalisms. A few results relative to exact expansions of the pressure are also presented.

3.1.1 The model

We consider a multicomponent system $\mathcal{S}$, with an arbitrary number of species made of point particles. Each particle of species α (an electron or a nuclei in practical applications) has a mass m_α and carries a charge e_α and a spin σ_α. Two charges e_α and e_β separated by a distance r interact instantaneously via the usual two-body Coulomb potential $e_\alpha e_\beta v_c(r)$ with $v_c(r) = 1/r$. The corresponding Hamiltonian for N particles enclosed in a box with volume Λ is

$$H_N = -\sum_i \frac{\hbar^2}{2m_i}\Delta_i + \frac{1}{2}\sum_{i\neq j}\frac{e_i e_j}{|\vec{r}_i - \vec{r}_j|} \tag{1}$$

where $i = \binom{k}{\alpha}$ is a double index, while k runs from 1 to the number N_α of charges of species α and α runs from 1 to the number n_s of species ($N = \sum_\alpha N_\alpha$). The boundary conditions which define H_N are of the Dirichlet type, i.e. the eigenwavefunctions of H_N vanish at the surface of the box. This non-relativistic Coulomb Hamiltonian is well-suited for practical applications where the mean velocity of the particles is small compared to the speed of light.

Let the system be in thermal equilibrium at temperature T ($\beta = 1/k_B T$). The grand-partition function of the finite system reads

$$\Xi_\Lambda = Tr_\Lambda \exp[-\beta(H_N - \sum_\alpha \mu_\alpha N_\alpha)] \tag{2}$$

where μ_α is the chemical potential of species α. In the definition (2), the trace Tr_Λ is taken over all the states satisfying the above boundary conditions and symmetrized according to the statistics of each species. Note that the total charge $\sum_\alpha e_\alpha N_\alpha$ carried by each of these states may be different from zero.

3.1.2 The Thermodynamic Limit

Lieb and Lebowitz (1972) have shown that the thermodynamic limit (TL)

https://doi.org/10.1017/S0252921100026312 Published online by Cambridge University Press

of the present system exists if and only if at least one species obeys Fermi statistics. The TL is defined as the infinite volume limit ($\Lambda \to \infty$), while the chemical potential μ_α and the temperature T are kept fixed. The existence of the TL means that the thermodynamic quantities relative to the infinite system have the right extensive properties. In particular, the bulk pressure P given through

$$\beta P = \lim_{TL} \frac{1}{\Lambda} \ln \Xi_\Lambda \tag{3}$$

is a well-behaved function of the intensive parameters μ_α and β which does not depend on the shapes of the finite boxes considered in the TL. If the fugacities $z_\alpha = \exp(\beta\mu_\alpha)$ are small enough (at given temperature), the system surely is in a fluid phase. The local density of any species α then becomes uniform in the TL and reduces to

$$\rho_\alpha = z_\alpha \frac{\partial}{\partial z_\alpha} \left[\lim_{TL} \frac{1}{\Lambda} \ln \Xi_\Lambda \right] |_\beta \tag{4}$$

Furthermore, the infinite system is locally neutral, i.e.

$$\sum_\alpha e_\alpha \rho_\alpha = 0 \tag{5}$$

for any set of fugacities. This is due to the fact that all the excess charges (associated to non-neutral states ($\sum_\alpha e_\alpha N_\alpha \neq 0$) go to the boundaries in order to minimize the electrostatic energy. Once the TL has been taken, these charges are rejected to infinity and the bulk region is neutral.

The existence of the TL is guaranteed by the combination of several phenomena. First, the most probable microscopic configurations can be organized in ensembles of finite neutral clusters which are weakly coupled because of screening. This physical idea can be formulated in a precise mathematical way with the help of the cheese theorem and of the harmonicity of the Coulomb potential (see Lieb (1976) for a review). Of course, this screening mechanism requires the presence of charges with opposite sign (otherwise the system explodes). Second, the classical collapse between two opposite charges at short distances is avoided by the uncertainty principle. The latter ensures that the quantum density matrix remains finite, and consequently integrable, at zero separations in configuration space. Third, the H-stability prevents the macroscopic collapse of all the matter into a big molecule. This property stipulates that the hamiltonian H_N in the infinite volume is bounded below by an extensive constant (i.e. the groundstate of H_N is bounded below by $cst \times N$). Dyson and Lenard (1967, 1968) have

https://doi.org/10.1017/S0252921100026312 Published online by Cambridge University Press

proved that the H-stability is enforced by Pauli's principle, which requires the presence of Fermions.

The existence of the TL implies the stability of matter with respect to electrostatic Coulomb interactions. It explains the usual aspect of the physical systems which can be reasonably described by the present model. Moreover, it justifies the calculation of bulk quantities in the infinite volume without any explicit consideration of boundary effects.

3.2 First Principles Formalisms

3.2.1 *Effective potential method*

This very general method, not specific to Coulomb systems, is due to Morita (1959). It consists in introducing an equivalent classical system made of point objects with many-body effective interactions. For the sake of simplicity, we expose this method in the framework of Maxwell-Boltzmann (MB) statistics and we just mention how the exchange effects due to Fermi or Bose statistics can be included in a straightforward way.

In configuration space, the MB grand-partition function reads

$$\Xi_{\Lambda}^{MB} = \sum_{N_\alpha=0}^{\infty} \prod_{\alpha} \frac{z_\alpha^{N_\alpha}}{N_\alpha!} (2\sigma_\alpha + 1)^{N_\alpha} \int_{\Lambda^N} \prod_i d\vec{r}_i \times < \vec{R}_N | \exp(-\beta H_N) | \vec{R}_N > \tag{6}$$

with $| \vec{R}_N >= \otimes_i | \vec{r}_i >$. In (6), the contributions of the spins reduce to the trivial degeneracy factors $(2\sigma_\alpha + 1)^{N\alpha}$ because H_N does not depend on the spins. The diagonal part $< \vec{R}_N | \exp(-\beta H_N) | \vec{R}_N >$ of the quantum density matrix can be always interpreted as a classical Boltzmann factor associated to an effective interaction φ_N such that

$$< \vec{R}_N | \exp(-\beta H_N) | \vec{R}_N >= \frac{1}{\prod_i (2\pi\lambda_i^2)^{3/2}} \exp\left(-\beta\varphi_N\right) \tag{7}$$

where $\lambda_i = (\beta\hbar^2/m_i)$ is the de Broglie wavelength associated to the i^{th} particle. Contrarily to the interaction part of H_N, φ_N does not reduce to a sum of two-body terms. This is a consequence of the non-commutativity between the kinetic and potential energies in quantum mechanics. However, it is convenient to split φ_N into a sum of two-body, three-body and higher order interactions. By specifying the identity (7) to the case of two particles i and j, one easily finds

https://doi.org/10.1017/S0252921100026312 Published online by Cambridge University Press

$$\varphi_2(\vec{r}_i,\vec{r}_j) = u_{ij}^{(2)} = -k_B T \ln\Big[(2\pi\lambda_i^2)^{3/2}(2\pi\lambda_j^2)^{3/2} \times < \vec{r}_i\vec{r}_j|\exp(-\beta H_2)|\vec{r}_i\vec{r}_j >\Big] \tag{8}$$

The total three-body effective interaction $\varphi_3(\vec{r}_i, \vec{r}_j, \vec{r}_k)$ between three particles i, j and k is then decomposed as

$$\varphi_3(\vec{r}_i,\vec{r}_j,\vec{r}_k) = u_{ij}^{(2)} + u_{jk}^{(2)} + u_{ik}^{(2)} + u_{ijk}^{(3)} \tag{9}$$

with

$$u_{ijk}^{(3)} = -k_B T \ln\Big\{ < \vec{r}_1\vec{r}_2\vec{r}_3|\exp(-\beta H_3)|\vec{r}_1\vec{r}_2\vec{r}_3 > / \Big[(2\pi\lambda_i^2)^{3/2} \times (2\pi\lambda_j^2)^{3/2}(2\pi\lambda_k^2)^{3/2} < \vec{r}_i\vec{r}_j|\exp(-\beta H_2)|\vec{r}_i\vec{r}_j > < \vec{r}_i\vec{r}_k|\exp(-\beta H_2)|\vec{r}_i\vec{r}_k >< \vec{r}_j\vec{r}_k|\exp(-\beta H_2)|\vec{r}_j\vec{r}_k >\Big]\Big\} \tag{10}$$

Similar decompositions of $\varphi_N\,(N > 3)$ in terms of the two-, three-, ..., N-body u-interactions can be found recursively. The insertion of these decompositions in (7) and use of the configurational expression (6) for Ξ_Λ^{MB} lead to

$$\Xi_\Lambda = \sum_{N_\alpha=0}^{\infty} \prod_\alpha z_\alpha{}^{N_\alpha} \frac{\big(2\sigma_\alpha+1\big)^{N_\alpha}}{(2\pi\lambda_\alpha^2)^{3N_\alpha/2} N_\alpha!} \int_{\Lambda^N} \prod_{i=1}^{N} d\vec{r}_i \exp\Big\{-\beta\Big[\sum_{i<j} u_{ij}^{(2)} + \sum_{i<j<k} u_{ijk}^{(3)} + \ldots\Big]\Big\}. \tag{11}$$

This identity shows that the MB grand-partition function of the quantum system $\mathcal{S}$ is identical to the one of an auxiliary classical system made of point objects interacting via two-, three-, ... and N-body effective interactions. For Fermi or Bose statistics, the same equivalence holds with effective u-interactions defined in terms of the symmetrized matrix elements of $\exp(-\beta H_N)$. The introduction of the above equivalent system allows to study the pressure, and consequently all the thermodynamic functions of $\mathcal{S}$, within the usual methods of classical statistical mechanics. However, we stress that the difficulties inherent to quantum mechanics rely in the determination of the many-body effective interactions. In the limit $\hbar \to 0$, $u_{ij}^{(2)}$

https://doi.org/10.1017/S0252921100026312 Published online by Cambridge University Press

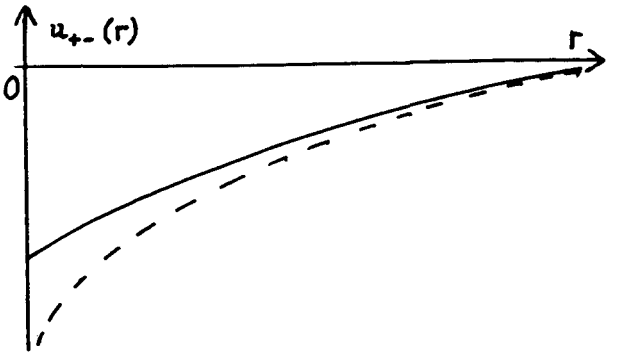

Fig. 1.1 Solid line : the effective-potential $u_{+-}^{(2)}(r)$ between two opposite charges $(+e)$ and $(-e)$; dashed line : the Coulomb potential $-e^2/r$.

goes to $e_i\, e_j\, v_c(|\vec{r}_i - \vec{r}_j|)$ while all the higher order effective interactions $u^{(N)}$ vanish. The effective-potential expression (11) then reduces to the classical grand-partition function of $\mathcal{S}$, as it should be.

The effective potential method has been first applied to quantum plasmas by Ebeling (1967) with the purpose of deriving low-density expansions of the thermodynamic functions. This method is indeed well-suited for such calculations for the following reason. By construction, the N-body effective interaction $u^{(N)}$ goes to zero for any large separation of its arguments. So the configurations where $u^{(N)}$ contributes to Ξ_Λ, are made of finite-size clusters which all contain at least N particles. This suggests that the contributions of $u^{(N)}$ to the pressure should be at least of order ρ^N (ρ is a generic notation for the particle densities). According to this simple rough argument, the density-expansion of the pressure up to the order ρ^N included can be calculated exactly by omitting all the effective interactions $u^{(M)}$ with $M > N$. In particular, Ebeling and coworkers (see references in the book by Kraeft et al. (1986)) performed calculations up to the order $\rho^{5/2}$ by keeping only the two-body effective interactions $u^{(2)}$. The potentials $u^{(2)}$ can be viewed as Coulomb interactions regularized at short distances. Indeed, at large distances $u_{ij}^{(2)}$ behaves as the Coulomb potential, i.e., $e_i\, e_j / |\vec{r}_i - \vec{r}_j|$, while $u_{ij}^{(2)}$ remains finite at zero separation because quantum diffraction smoothes out the 1/r-singularity at the origin. For fixing ideas, we have drawn in Figure 1 the effective interaction $u_{+-}^{(2)}(r)$ between two oppposite charge $(+e)$ and $(-e)$ separated by a distance r.

The auxiliary classical system with the two-body Coulomb-like interactions $u^{(2)}$ can be studied by various standard methods. In particular, the

density-expansion of the pressure may be readily obtained from Abe-Meeron diagrammatics. The corresponding graphs follow from systematic resummations of the convolution chains in the genuine Mayer graphs built with bonds $(\exp[-\beta u^{(2)}] - 1)$. This procedure eliminates the divergencies induced by the Coulomb long-range part of $u^{(2)}$, and make an integrable screened potential appear. The definition of the screened potential in terms of $u^{(2)}$ is identical to the one of the familiar Debye-Hückel potential in terms of the 1/r-Coulomb potential.

As it will be discussed with more details in Section 5, and contrarily to what was expected, the density expansions calculated by the above authors are correct only up to the order ρ^2 included. In fact, the contributions of the three-body effective interactions $u^{(3)}$ are of order $\rho^{5/2}$ instead of ρ^3. This is due to the fact that $u^{(3)}$ is long ranged, i.e., not integrable at large distances. Of course the exact expression of the virial coefficient of order $\rho^{5/2}$ might be obtained by the above method via a proper inclusion of the three-body effective interactions.

3.2.2 *Many-Body Perturbation*

This method consists in a perturbative treatment of the interaction part of the Hamiltonian H_N given by (1). It allows systematic expansions of the equilibrium quantities in powers of the charges which characterize the strength of Coulomb interactions. The formalism is carefully presented in the book by Fetter and Walecka (1971). Here, we just describe the main steps of the method.

The perturbative expansion is carried out in the framework of the grand-canonical ensemble, at fixed temperature and fugacities (the corresponding expansion in the canonical ensemble is more cumbersome because of the so-called 1/N tails). The key starting identity is the Dyson series which represent the quantum Gibbs factor (i.e. the density matrix) as

$$\exp\left(-\beta H_N\right) = \exp\left(-\beta H_0\right)\left\{1 + \sum_{n=1}^{\infty} \frac{(-1)^n}{n!} \times \int_0^\beta d\tau_1 \ldots \int_0^\beta d\tau_n T_\tau\left[V_{\tau_1}^0 \ldots V_{\tau_n}^0\right]\right\} \tag{12}$$

where H_0 and V are the kinetic and interaction parts of H_N respectively. Moreover, V_τ^0 is the imaginary-time evoluted operator.

https://doi.org/10.1017/S0252921100026312 Published online by Cambridge University Press

$$V_\tau^0 = \exp(\tau H_0) V \exp(-\tau H_0) \tag{13}$$

and T_τ is the familiar T-product which ranges all operators from left to right which decreasing "times" τ. The insertion of the Dyson series (12) in the trace (2) leads to the required perturbative representation of any equilibrium function of $\mathcal{S}$. Each term in these perturbative series obviously reduces to a statistical equilibrium average $< \ldots >_0$ calculated with the free-particle Gibbs measure $\exp\left[-\beta(H_0 - \sum_\alpha \mu_\alpha N_\alpha)\right] / \Xi_{\Lambda,0}$. For instance, the V-expansion of the pressure given by Eq. (3) involves

$$< T_\tau \left[V_{\tau_1}^0 \ldots V_{\tau_n}^0 \right] >_0 \tag{14}$$

Since V is diagonal in configuration space and reduces to a sum of two body terms, one easily guesses that the above averages may be expressed as multiple spatial integrals over products of two-body interactions weighted by equilibrium configuration distributions relative to the reference system $\mathcal{S}_0$. Moreover these distributions reduce to products of one-body terms because the particles of $\mathcal{S}_0$ are not coupled together.

The precise structure of the perturbative terms, like (14) for instance, might be determined via suitable insertions of the familiar configurational Slater sums. However, this leads, at high orders in V, to complicated counting problems of permutations. In order to circumvent these difficulties linked to statistics, it is particularly convenient to introduce the second quantization representation defined in terms of the operators $\Psi_\alpha(\vec{r}\sigma^z)$ or $\Psi_\alpha^\dagger(\vec{r}\sigma^z)$ which respectively annihilates or creates one particle of species α at position $\vec{r}$ with spin σ^z along a given z-axis. In the framework of the grand-canonical ensemble, this representation is in fact quite appealing since the total number of particles is not fixed. Furthermore, the bosonic or fermionic nature of each species is automatically taken into account via the commutation or anticommutation relations,

$$\Psi_\alpha^\dagger(\vec{r},\sigma^z)\Psi_\alpha(\vec{r}',\sigma^{z\prime}) \pm \Psi_\alpha(\vec{r}',\sigma^{z\prime})\Psi_\alpha^\dagger(\vec{r},\sigma^z) = \delta_{\sigma^z,\sigma^{z\prime}} \times \delta(\vec{r}-\vec{r}')$$
$$\Psi_\alpha^\dagger(\vec{r},\sigma^z)\Psi_\alpha^\dagger(\vec{r}',\sigma^{z\prime}) \pm \Psi_\alpha^\dagger(\vec{r}',\sigma^{z\prime})\Psi_\alpha^\dagger(\vec{r},\sigma^z) = 0$$
$$\Psi_\alpha(\vec{r},\sigma^z)\Psi_\alpha(\vec{r}',\sigma^{z\prime}) \pm \Psi_\alpha(\vec{r}',\sigma^{z\prime})\Psi_\alpha(\vec{r},\sigma^z) = 0$$

while two operators associated to different species always commute. The second-quantized expressions of the operators of interest read

https://doi.org/10.1017/S0252921100026312 Published online by Cambridge University Press

$$H_0 = \sum_{\alpha} \sum_{\sigma_z=-\sigma_\alpha}^{\sigma_\alpha} \int d^3\vec{r} \Psi_\alpha^\dagger(\vec{r},\sigma^z)\left[-\frac{\hbar^2}{2m_\alpha}\Delta\right]\Psi_\alpha(\vec{r},\sigma^z) \tag{15}$$

$$V = \frac{1}{2}\sum_{\alpha,\beta}\sum_{\sigma^z,\sigma^{z'}} \int d^3\vec{r}\int d^3\vec{r}' \Psi_\alpha^\dagger(\vec{r},\sigma^z)\Psi_\beta^\dagger(\vec{r}',\sigma^{z'}) \times e_\alpha e_\beta v_C(|\vec{r}-\vec{r}'|)\Psi_\beta(\vec{r}',\sigma^{z'})\Psi_\alpha(\vec{r},\sigma^z) \tag{16}$$

$$N_\alpha = \sum_{\sigma^z}\int d^3\vec{r}\Psi_\alpha^\dagger(\vec{r},\sigma^z)\Psi_\alpha(\vec{r},\sigma^z) \tag{17}$$

(now N_α is the number-operator which counts the particles of species α). The averages like (14) appearing in the V-expansions then involve traces over the Fock space of the products of $(\Psi^\dagger)^0_{\tau_i}$ and $(\Psi^\dagger)^0_{\tau_j}$ weighted by the free-particles measure

$$\frac{1}{\Xi_{\Lambda,0}}\exp\left\{-\beta\sum_\alpha\sum_{\sigma^z}\int d^3\vec{r}\left[\Psi_\alpha^\dagger(\vec{r},\sigma^z)\left(-\frac{\hbar^2}{2m_\alpha}\Delta\right)\Psi_\alpha(\vec{r},\sigma^z) - \mu_\alpha\Psi_\alpha^\dagger(\vec{r},\sigma^z)\Psi_\alpha(\vec{r},\sigma^z)\right]\right\} \tag{18}$$

Since the measure (18) is Gaussian in the Ψ's, and since all the Ψ's commute or anticommute except for c-numbers, the above traces can be calculated with help of Wick's theorem. Similarly to the formula which relates any moment for a Gaussian distribution of real variables to the covariances, the free-particle average of any product of Ψ's is identically equal to the sum over the products of all the possible corresponding two-operators contractions. The sole non-vanishing contractions are those which conserve the number of particles of each species. They reduce to the finite-temperature one-particle Green's functions of $\mathcal{S}_0$, i.e.

$$G_{\alpha,0}(\vec{r}',\sigma^z,\tau';\vec{r},\sigma^z,\tau) = < T_\tau\left[\left(\Psi_\alpha^\dagger(\vec{r},\sigma^z)\right)^0_\tau\left(\Psi_\alpha(\vec{r}',\sigma^z)\right)^0_{\tau'}\right] >_0 \tag{19}$$

The second-quantization analysis of the V-expansions provides well-defined rules for interpreting each term as a Feynman graph similar to those which appear in field theory. Roughly speaking, the graphs are made of one-particle fermionic or bosonic oriented loops connected by two-body interaction lines. The two points linked by a given interaction line are affected of the same "time" τ_i. They may belong either to the same loop or to different

https://doi.org/10.1017/S0252921100026312 Published online by Cambridge University Press

loops. Each loop contains an arbitrary number n_L of points $\vec{r}_i$ at time τ_i. Its statistical weight is given by the product

$$\prod_{i=1}^{n_L} G_{\alpha,0}(\vec{r}_i\sigma^z\tau_i, \vec{r}_{i+1}\sigma_z\tau_{i+1}) \tag{20}$$

of the free-particle Green's function connecting two successive points on the loop ($\vec{r}_{n_{L+1}} = \vec{r}_1$ and $\tau_{n_{L+1}} = \tau_1$). The weight of a loop containing only one point reduces to

$$G_{\alpha,0}(\vec{r}_1, \sigma^z, \tau_1; \vec{r}_1, \sigma^z, \tau_1) = \frac{1}{(2\pi)^3} \int d\vec{k} \frac{z_\alpha \exp\left(-\beta\frac{\hbar^2k^2}{2m_\alpha}\right)}{\left[z_\alpha \exp\left(-\beta\frac{\hbar^2k^2}{2m_\alpha}\right) \pm 1\right]} \tag{21}$$

which is nothing but $\rho_{\alpha,0} / (2\sigma_\alpha + 1)$ with $\rho_{\alpha,0}$ the particle density of $\mathcal{S}_0$ (note that $\rho_{\alpha,0}$ is different from the particle density ρ_α of the interacting system $\mathcal{S}$). In general, for the considered physical quantities, each graph is connected. For instance, in the case of the pressure, the disconnected graphs which appear in the expansion of Ξ_Λ are eliminated in the corresponding logarithm. In Figures (2a) and (2b), we have drawn two typical graphs which contribute to this quantity. The graph (2a) is of the exchange type since the interaction line links two points on the same loop. The graph (2b) is of the direct type since the interaction lines link points belonging to distinct loops. Note that if one sets $\hbar \to 0$, all the exchange graphs disappear while all the loops are contracted in single points with statistical weights $(2\sigma_\alpha + 1)z_\alpha / (2\pi\lambda_\alpha^2)^{3/2}$. One then recovers the classical graphs which can be inferred from the familiar Mayer graphs by expanding the Mayer bonds ($\exp[-\beta e_i e_j v_c(r_{ij}] - 1$) in Taylor series with respect to v_c. The general structure of the Feynman graphs does not depend on the precise nature of the two-body interactions. In the present Coulomb case, part of these graphs (involving direct contributions) diverge because $v_c(r)$ is not integrable at large-distances. These long-range divergencies are similar to the ones which appear in the classical Mayer graphs. Like in the purely classical case, the divergencies in the pressure are eliminated by summing together the ring structures, as shown by Montroll and Ward (1958). For instance the divergent contribution of the graph (2b) is combined to the divergent contributions of all the ring graphs made of n loops connected by n interation lines with $n \geq 3$ (an example of such ring graphs is shown in Figure 3). The sum of all these ring contributions is finite. For the particle correlations, one must resum chain structures instead of rings (see

https://doi.org/10.1017/S0252921100026312 Published online by Cambridge University Press

Fig. 1.2 a, 1.2b Two Feynman graphs which contribute to the e^2-expansion of the pressure. Big oriented circles : fermionic or bosonic loops ; dashed lines : two-body interactions connecting pairs of points (small black circles) on the loops.

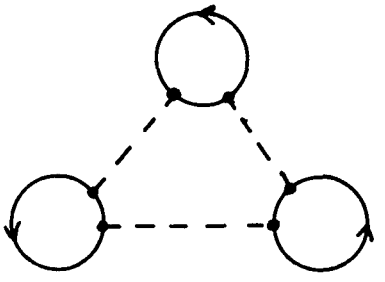

Fig. 1.3 A typical ring graph.

e.g. Cornu and Martin (1991)). All these mathematical recipes reflect the screening of the bare Coulomb interaction via many-body collective effects. The expansion parameter in the above perturbative series is the charge e, where e is a generic notation for the charges of the particles. The lowest order correction to the pressure P_0 of the free gas $\mathcal{S}_0$ is given by the exchange graph (2a) which is of order e^2 (the direct contribution of order e^2 vanishes because of overall neutrality). The next correction is not of order e^4 as a consequence of the long-range divergencies which prevent the pressure to be an analytic function of e^2. This correction is given by the sum of all the ring graphs analogous to (2b) and (3) (physically, this contribution corresponds to the RPA mean-field approximation). The analytic evaluation

https://doi.org/10.1017/S0252921100026312 Published online by Cambridge University Press

of the ring sum for any temperature and fugacities is quite cumbersome. To our knowledge, it has been done explicitely in two cases.

First, for an electron gas (one-component plasma of fermions) at zero-temperature, Montroll and Ward (1958) have shown that the ring contribution to the internal energy per particle E/N is of order $e^4 \ln e^2$. In fact, they recover the e^2-expansion.

$$\frac{E}{N} = \frac{3^{5/3}\pi^{4/3}\hbar^2}{10m}\rho^{2/3} - \frac{3^{4/3}}{4\pi^{1/3}}\rho^{1/3}e^2 + \frac{(1-\ln 2)}{\pi^2}\frac{m}{\hbar^2}e^4 \ln\left(\frac{e^2 m}{\hbar^2 \rho^{1/3}}\right) + 0(e^4) \tag{22}$$

first derived by Gell-Mann and Brueckner (1957) in the framework of the adiabatic perturbation-switching formalism (the graphs introduced in this perturbative treatment of the ground state turn out to be quite similar to those described above). The expansion (22) can be rewritten in terms of the single dimensionless parameter r_s defined as the ratio of the mean interparticle distance $a = (3/4\pi\rho)^{1/3}$ by the Bohr radius $a_B = \hbar^2 / me^2$. The appearance of r_s is quite natural since r_s is proportional to the ratio of the mean Coulomb energy ($\sim \rho^{1/3}$) divided by the Fermi kinetic energy ($\sim \rho^{2/3}$). The expansion (22) should converge for small values of r_s, i.e., at high densities. It can be also viewed as an asymptotic expansion in inverse powers of the density.

The second analytic evaluation of the ring contribution has been performed in the high-temperature limit. This contribution then becomes of order e^3 and leads to the well-known classical Debye-term $-\kappa_D^3 / (24\pi)$ with $\kappa_D = (4\pi\beta \sum_\alpha e_\alpha^2 \rho_\alpha)^{1/2}$. The e^2-expansion should be quite appropriate at high temperatures since the mean Coulomb energy e^2/a then becomes small compared to the thermal kinetic energy $k_\beta T$. Consequently, a natural by-product of these perturbative series is the derivation of high-temperature expansions. However, the reorganization of the e^2-series in β-series is not straightforward because both expansions involve several independent dimensionless parameters. Indeed, in addition to the coupling parameter $\beta e^2/a (\sim \beta)$ which measures the strength of Coulomb interactions, they depend on the quanticity parameter $\lambda/a (\sim \beta^{1/2})$ which controls diffraction and degeneracy effects. The β-expansion of βP up to the order $\beta^{5/2}$ has been calculated by De Witt (1966) in the framework of Maxwell-Boltzmann

https://doi.org/10.1017/S0252921100026312 Published online by Cambridge University Press

statistics. Keeping only the free term βP_0 and the ring sum, he found

$$\beta P = \sum_\alpha \rho_\alpha - \frac{1}{24\pi}\left(4\pi \sum_\alpha e_\alpha^2 \rho_\alpha\right)^{3/2} \beta^{3/2} + \frac{\pi^{3/2}}{2^{5/2}} \sum_{\alpha,\beta} \frac{e_\alpha^2 e_\beta^2 \hbar}{m_{\alpha\beta}^{1/2}} \rho_\alpha \rho_\beta \beta^{5/2} + O(\beta^3 \ln \beta) \tag{23}$$

Notice that the exchange effects will give terms of orders $\beta^{3/2}$ (the usual Fermi or Bose ideal term), β^2 (contribution from the exchange graph (2a)), $\beta^{5/2}$ and so on. Moreover, the $\beta^{5/2}$-term arising from the β-expansion of the ring sum is proportional to $\hbar$. In fact, the higher order interaction terms in (23) involve any integer power of $\hbar$, even or odd, positive or negative. This general singular structure with respect to $\hbar$ of the β-expansions hold in particular for the OCP. In that case, the pressure (and the other thermodynamic functions) may be also represented by the familiar Wigner-Kirkwood (WK) expansion in powers of $\hbar^2$ around the classical limit (the WK expansion cannot be used for a multicomponent system because the collapse of opposite charges makes the classical limit singular). One then concludes that the β- and WK-expansions do not coincide. As argued by De Witt (1962), this a priori surprising result can be interpreted by noting that, in the high-temperature limit, the de Broglie wavelength $\lambda = (\beta\hbar^2 / m)^{1/2}$ becomes much larger than the Landau length $l = \beta e^2$ which is a classical average range of the Coulomb interactions. The validity of the WK-expansion requires, roughly speaking, $\lambda \ll l$, a criterion which is satisfied, on the contrary, at rather low temperatures.

The e^2-expansions also constitute the starting point of the so-called fugacity expansions introduced by Rogers (1974). This author proposed a classical treatment of the ring resummations, combined to additional resummations of Ladder graphs of the type shown in Figure (4) with an arbitrary number of interaction lines. The latter amount to introduce Coulomb thermal propagators at short distances in order to take into account the contributions of bound states. In this procedure, some terms are left over since they are expected to be quantitatively small in the physical regimes considered by the author (i.e. at moderately high densities where complex entities made of several charges may be formed). The corresponding calculations are reviewed in the present volume.

https://doi.org/10.1017/S0252921100026312 Published online by Cambridge University Press

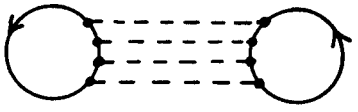

Fig. 1.4 A typical Ladder graph.

3.3 The Feynman-Kac Representation

3.3.1 *The case of one particle*

For the sake of pedagogy, we first illustrate the Feynman-Kac representation for one particle with mass m submitted to an external potential $V(\vec{r})$. According to the original path integral formulation introduced by Feynman (1965), the diagonal matrix element of $\exp[-\beta(-\frac{\hbar^2}{2m}\Delta + V)]$ reads

$$< \vec{r}| \exp\left[-\beta(-\frac{\hbar^2}{2m}\Delta + V)\right] |\vec{r}> = \sum_{\text{all paths}} \exp\left(-\frac{S(\vec{r}(t))}{\hbar}\right) \qquad (24)$$

where $S(\vec{r}(t))$ is the classical action in the potential $-V$,

$$S(\vec{r}(t)) = \int_0^{\beta\hbar} dt \left\{ \frac{m}{2}\left[\frac{d\vec{r}(t)}{dt}\right]^2 + V(\vec{r}(t)) \right\} \qquad (25)$$

for a path $\vec{r}(t)$ going from $\vec{r}$ to $\vec{r}$ in a "time" $\beta\hbar$. The summation in (24) is taken over all such paths. The variable changes $t = s\beta\hbar$ and $\vec{r}(t) = \vec{r} + \lambda\vec{\xi}(s)$ with $\lambda = (\beta\hbar^2/m)^{1/2}$ in (24) and (25) lead to the so-called Feynman-Kac (FK) representation (see e.g. B. Simon (1979))

$$< \vec{r}| \exp\left[-\beta(-\frac{\hbar^2}{2m}\Delta + V)\right] |\vec{r}> = \frac{1}{(2\pi\lambda^2)^{3/2}} \int \mathcal{D}(\vec{\xi}) \exp[-\beta V^\star(\vec{r}, \vec{\xi})] \qquad (26)$$

with

$$V^\star(\vec{r}, \vec{\xi}) = \int_0^1 ds V(\vec{r} + \lambda\vec{\xi}(s)) \qquad (27)$$

https://doi.org/10.1017/S0252921100026312 Published online by Cambridge University Press

The factor $\exp[-\beta V^*(\vec{r},\vec{\xi})]$ obviously arises from the potential part of the action S. The corresponding kinetic factor, i.e. $\exp[-\frac{1}{2}\int_0^1 d\,s\,\dot{\vec{\xi}}^2(s)]$, is absorbed in the normalized Gaussian measure $\mathcal{D}(\vec{\xi})$ which defines the functional integration over all the dimensionless Brownian bridges $\vec{\xi}(s)$ subjected to the constraint $\vec{\xi}(0)=\vec{\xi}(1)=\vec{0}$. This measure is intrinsic, i.e. independent of all the physical parameters, and its covariance is given by

$$\int \mathcal{D}(\vec{\xi})\xi_\mu(s)\xi_\nu(t) = \delta_{\mu\nu} \times \begin{cases} s(1-t), & s \le t \\ t(1-s), & t \le s \end{cases} \tag{28}$$

It is very natural to interpret $\exp[-\beta V^*(\vec{r},\vec{\xi})]$ as the Boltzmann factor associated to a classical closed filament located at $\vec{r}$ and with shape parametrized by $\vec{\xi}(s)$. The potential V^* seen by this filament is the average of the genuine potential seen by the particle when it runs over the line $\vec{r}+\lambda\vec{\xi}(s)$. The FK representation (26) stipulates that the Gibbs factor for the quantum point particle exactly reduces to the shape-average of this Boltzmann factor with the Gaussian measure $\mathcal{D}(\vec{\xi})$. The de Broglie wavelength λ controls the typical size of a filament : roughly speaking, the statistical weight of a filament with size R behaves as $\exp(-R^2/\lambda^2)$. Note that the classical limit of the density matrix is immediately obtained from (26) by replacing V^* by $V(\vec{r})$: in this limit, λ goes to zero and the spatial extension of the filaments can be neglected in the calculation of $V^*(\vec{r},\vec{\xi})$.

3.3.2 *The system $\mathcal{S}$ with Maxwell-Boltzmann statistics*

First, we only consider MB statistics. The corresponding grand-partition function Ξ_Λ^{MB} of $\mathcal{S}$ is given by the space-configurational expression (6). Similarly to the expression (26), the FK representation of the diagonal matrix elements of $\exp(-\beta H_N)$ reads

$$\begin{aligned} <\vec{R}_N|\exp(-\beta H_N)|\vec{R}_N> = \prod_\alpha \frac{1}{(2\pi\lambda_\alpha^2)^{3N_\alpha/2}} \int \prod_i \mathcal{D}(\vec{\xi}_i) \\ \times \exp\left[-\frac{\beta}{2}\sum_{i\neq j} e_i e_j \int_0^1 ds v_c(|\vec{r}_i+\lambda_i\vec{\xi}_i(s)-\vec{r}_j-\lambda_j\vec{\xi}_j(s)|)\right] \end{aligned} \tag{29}$$

where each Brownian bridge $\vec{\xi}_i(s)$ parametrizes the trajectory of the i^{th} particle in the genuine Feynman path integral, and is distributed according to the intrinsic Gaussian measure defined above. This representation suggests to introduce the following auxiliary classical system $\mathcal{S}^*$ made of closed

https://doi.org/10.1017/S0252921100026312 Published online by Cambridge University Press

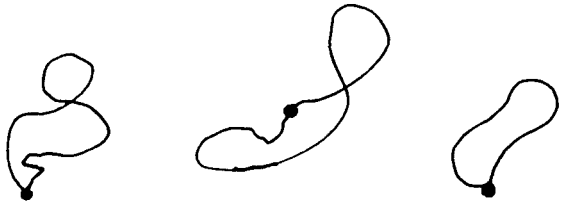

Fig. 1.5 A few closed filaments which belong to $\mathcal{S}^*$. The small black circles represent the positions of the filaments, while the closed curves attached to each of them represent their shapes parametrized by $\lambda\vec{\xi}(s)$.

filaments interacting via two-body forces. Each filament is characterized by its spatial position $\vec{r}$ and two internal degrees of freedom, the dimensionless path $\vec{\xi}(s)$ associated to its shape and the species index α which specifies its spatial extension λ_α and the strength e_α of its coupling with the other filaments. We note $\mathcal{E} = (\alpha, \vec{r}, \vec{\xi})$ the state of such a filament. Two filaments in states $\mathcal{E}$ and $\mathcal{E}'$ interact via the two-body potential $e_\alpha e_{\alpha'} v(\mathcal{E}, \mathcal{E}')$ with

$$v(\mathcal{E}, \mathcal{E}') = \int_0^1 ds v_c(|\vec{r} + \lambda_\alpha \vec{\xi}(s) - \vec{r}' - \lambda_{\alpha'} \vec{\xi}'(s)|) \tag{30}$$

This potential is different from the electrostatic interaction energy between two uniformly charged filaments, because the average of v_c is taken over positions at the same "time" s. However, it reduces to the Coulomb potential at large distances, i.e.

$$v(\mathcal{E}, \mathcal{E}') \sim 1/|\vec{r} - \vec{r}'| \quad \text{when} \quad |\vec{r} - \vec{r}'| \to \infty \tag{31}$$

since the filaments can then be replaced by points. A few filaments are drawn in Figure 5.

The insertion of the FK representation (29) in the space-configurational expression (6) of Ξ_Λ^{MB} leads to a sum over the states of $\mathcal{S}^*$ weighted by Boltzmann factors associated to the filaments interactions. In this sum, it is quite natural to define the phase-space measure $d\mathcal{E}$ for a filament as $d\mathcal{E} = "d\alpha" d\vec{r} \mathcal{D}(\vec{\xi})$ and to set $z(\mathcal{E}) = (2\sigma_\alpha + 1) z_\alpha / (2\pi\lambda_\alpha^2)^{3/2}$ for its fugacity. The above sum is then identified as the grand-partition function Ξ_Λ^* of $\mathcal{S}^*$, i.e.

https://doi.org/10.1017/S0252921100026312 Published online by Cambridge University Press

$$\Xi_\Lambda^{MB} = \Xi_\Lambda^\star = \sum_{N=0}^{\infty} \frac{1}{N!} \int \prod_{k=1}^{N} d\mathcal{E}_k z(\mathcal{E}_k) \prod_{k<l} [1 + f(\mathcal{E}_k, \mathcal{E}_l)], \tag{32}$$

where $f(\mathcal{E}_k, \mathcal{E}_l)$ is the Mayer-bond associated to $v(\mathcal{E}_k, \mathcal{E}_l)$,

$$f(\mathcal{E}_k, \mathcal{E}_l) = \exp[-\beta e_{\alpha_k} e_{\alpha_l} v(\mathcal{E}_k, \mathcal{E}_l)] - 1. \tag{33}$$

The identity (32) exemplifies the equivalence between the quantum system $\mathcal{S}^{MB}$ and the classical system $\mathcal{S}^*$ for studying equilibrium properties. In $\mathcal{S}^*$, the quantum mechanical aspect of $\mathcal{S}^{MB}$ is hidden in the complex nature of the filaments. In fact, these extended objects describe quantum fluctuations of the point particles. In the effective-potential method, the auxiliary classical system is still made of point objects while the quantum effects are taken into account in the two-body and higher order effective interactions. Here, we stress that the interactions between the filaments are strictly of the two-body type.

3.3.3 *Inclusion of Fermi or Bose statistics*

In order to take into account the exchange effects due to Fermi or Bose statistics, we express the trace (2) over the properly symmetrized states $|\vec{R}_N \sigma_N >_s$ in configuration and spin spaces. These states are defined via the usual Slater sums

$$|\vec{R}_N \sigma_N^z >_S = \frac{1}{\prod_\alpha (N_\alpha!)^{1/2}} \sum_{\mathcal{P}_\alpha} \prod_\alpha \epsilon_\alpha(\mathcal{P}_\alpha) \otimes_i |\vec{r}_{\mathcal{P}_\alpha(i)} \sigma^z_{\mathcal{P}_\alpha(i)} > \tag{34}$$

In (33), $\mathcal{P}_\alpha$ is a permutation of $(1 \ldots N_\alpha)$, $\mathcal{P}_\alpha(i) = (\mathcal{P}_\alpha(k), \alpha)$, and $\epsilon_\alpha(\mathcal{P}_\alpha)$ is either 1 if the particles of species α are bosons (σ_α integer) or the signature (± 1) of $\mathcal{P}_\alpha$ in the fermionic case (σ_α half-integer). Furthermore, $\otimes$ means a tensioral product over the one-body states $|\vec{r}\sigma^z>$ describing a particle localized at $\vec{r}$ with the projection of its spin along a given z-axis equal to

https://doi.org/10.1017/S0252921100026312 Published online by Cambridge University Press

σ^z (σ^z may take $(2\,\sigma_\alpha + 1)$ values). Using (34), we obtain

$$\Xi_\Lambda = \sum_{N_\alpha=0}^{\infty} \frac{\prod_\alpha z_\alpha^{N_\alpha}}{[\prod_\alpha (N_\alpha!)]^2} \times \sum_{\mathcal{P}_\alpha, \mathcal{P}'_\alpha} \prod_\alpha \epsilon_\alpha(\mathcal{P}_\alpha)\epsilon_\alpha(\mathcal{P}'_\alpha) \sum_{\{\sigma_i^z\}} \prod_i < \sigma^z_{\mathcal{P}'_\alpha(i)} | \sigma^z_{\mathcal{P}_\alpha(i)} > \times \int_{\Lambda^N} \prod_i d\vec{r}_i < \vec{r}_{\mathcal{P}'_\alpha(i)} | \otimes_i | \exp(-\beta H_N) | \otimes_i | \vec{r}_{\mathcal{P}_\alpha(i)} > \quad (35)$$

Since the hamiltonian H_N (equation (1)) does not depend on the spins, the spin-part of the matrix elements contributes the trivial degeneracy factor $\sum_{\sigma_i^z} \prod_i < \sigma^z_{\mathcal{P}'_\alpha(i)} | \sigma^z_{\mathcal{P}_\alpha(i)} >$ which only depends on the pairs of permutations $(\mathcal{P}_\alpha, \mathcal{P}'_\alpha)$.

The Slater-sum representation (35) of Ξ_Λ alows a natural identification of the exchange effects. Indeed, the "square" terms ($\mathcal{P}_\alpha = \mathcal{P}'_\alpha$ for any α), where the diagonal matrix elements of $\exp(-\beta H_N)$ in configuration space appear, obviously correspond to MB statistics. A "rectangle" term ($\mathcal{P}_\alpha \neq \mathcal{P}'_\alpha$ for at least one species) involves the exchange of n particles ($n \geq 2$). The corresponding matrix elements of $\exp(-\beta H_N)$ are off-diagonal with respect to the positions of the exchanged particles. The structure of the FK representation of these off-diagonal matrix elements can be interpreted in two ways which lead to different treatments of the exchange contributions.

A first possible interpretation consists in introducing opened filaments $\mathcal{F}_{kl}^\alpha$ associated to the exchange of a particle α from position $\vec{r}_k$ to position $\vec{r}_l$. The shape of $\mathcal{F}_{kl}^\alpha$ is parametrized by

$$\vec{\omega}_{kl}^\alpha(s) = (1-s)\vec{r}_k + s\vec{r}_l + \lambda_\alpha \vec{\xi}(s) \quad (36)$$

which describes a path of the exchanged particle in the genuine Feynman path integral ($\vec{\omega}_{kl}(0) = \vec{r}_k$ and $\vec{\omega}_{kl}(1) = \vec{r}_l$). The above closed filaments $\mathcal{E}$ are again associated to the non-exchanged particles. For instance, if one considers the off-diagonal matrix element

$$< \vec{r}_2\vec{r}_1\vec{r}_3 \ldots \vec{r}_N | \exp(-\beta H_N) | \vec{r}_1\vec{r}_2\vec{r}_3 \ldots \vec{r}_N > \quad (37)$$

which corresponds to the exchange of two particles, there appear two opened filaments $\mathcal{F}_{12}^\alpha$ and $\mathcal{F}_{21}^\alpha$ and (N-2) closed filaments $\mathcal{E}_3$,..., $\mathcal{E}_N$. This situation is illustrated in Figure 6. By collecting together all the contributions with the same finite number n of exchanged particles, we are then left with a problem of impurities, the n opened filaments, immersed in the bath $\mathcal{S}^*$ of closed

https://doi.org/10.1017/S0252921100026312 Published online by Cambridge University Press

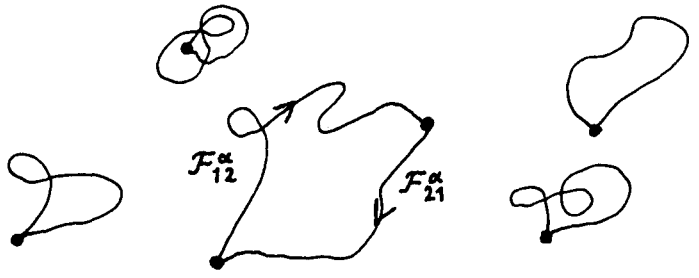

Fig. 1.6 Two opened filaments $\mathcal{F}_{12}^{\alpha}$ and $\mathcal{F}_{21}^{\alpha}$ surrounded by closed filaments of $\mathcal{S}^*$.

filaments. This inhomogeneous situation can be dealt with along standard perturbative techniques where the reference system is the homogeneous bath $\mathcal{S}^*$ described in section 3.2.

The second interpretation of the exchange contributions is due to Brydges (private communication). Any permutation of n objects, which characterizes the exchange of n particles, is the product of p cycles with $p < n$. Therefore, the corresponding n opened filaments may be always viewed as a set of p closed filaments. Each of these new closed filaments is made of q opened filaments, $q > 1$, and will be noted $\mathcal{E}^{(q)}$. It can be associated to a closed path described in a "time" $q\beta\hbar$. For instance, in the above example the union of $\mathcal{F}_{12}^{\alpha}$ and $\mathcal{F}_{21}^{\alpha}$ gives raise to $\mathcal{E}^{(2)}$. Therefore, the whole Slater representation (35) of Ξ_Λ is identified as the grand-partition function of a mixture of classical closed filaments $\mathcal{E}^{(q)}$ with q = 1,2,3...∞ (the $\mathcal{E}^{(1)}$'s are the closed filaments $\mathcal{E}$ introduced in section 3.2). The typical size of $\mathcal{E}^{(q)}$ depends on the "time" $q\beta\hbar$. Its activity incorporates a self-energy term arising from two-body interactions of the type (30) between the opened filaments which constitute $\mathcal{E}^{(q)}$. In the present approach, the MB and exchange effects are treated on an equal footing, while the previous interpretation leads to a perturbative treatment of the exchange contributions.

3.3.4 *Possible applications*

Within the above equivalences which follow from the FK representation, the equilibrium properties of the quantum system $\mathcal{S}$ can be studied by applying the usual methods of classical statistical mechanics to $\mathcal{S}^*$. Indeed, the system of closed filaments is isomorphic to an ordinary classical system

https://doi.org/10.1017/S0252921100026312 Published online by Cambridge University Press

of point objects with two-body interactions. In $\mathcal{S}^*$, the position $\vec{r}$ is replaced by the generalized coordinate $\mathcal{E}$. The familiar calculation rules remain unchanged, apart from this simple substitution, because all the quantities of $\mathcal{S}^*$ behave as commuting c-numbers (the operatorial structure of quantum mechanics "disappears" in the FK representation).

The familiar Mayer series can be extended to $\mathcal{S}^*$. For systems with short-range forces, Ginibre (1971) proved the convergence of the activity expansions by exploiting the classical structure of the Mayer-like graphs. For the present Coulomb systems, the Mayer-like series for $\mathcal{S}^*$ constitute a powerful tool in the systematic derivation of density-expansions (see Section 4). Aside from these exact calculations, one might introduce approximate methods by extending well-known integral equations (like HNC) to the correlations of $\mathcal{S}^*$ (see e.g. Chandler (1981) for a review relative to systems with short-range forces). Although such extensions do not cause any trouble at a formal level, we stress that the explicit calculations might be rather difficult because of the functional integrations over the shapes of the filaments.

3.4 Virial-Like Expansions

Like in the classical case, all the above Mayer-like graphs diverge because of the long-range Coulombic nature of the filament-filament potential. Alastuey, Cornu and Perez (1993) have shown that the corresponding series can be reorganized in series of finite resummed graphs. In this section, we just sketch the main steps of their method. First of all, they consider only MB statistics and the resummation procedure is applied to the Ursell function $h(\mathcal{E}_a, \mathcal{E}_b)$ of $\mathcal{S}^*$. The density expansions of the MB thermodynamic functions of $\mathcal{S}^{MB}$ are then evaluated via standard identities. The exchange effects are included perturbatively within the impurities approach exposed in Section 3.3.

3.4.1 *Diagrammatic resummations*

The two-point Ursell function $h(\mathcal{E}_a, \mathcal{E}_b)$ of $\mathcal{S}^*$ is defined as usual by

$$\rho(\mathcal{E}_a)\rho(\mathcal{E}_b)h(\mathcal{E}_a,\mathcal{E}_b) = z(\mathcal{E}_a)z(\mathcal{E}_b)\lim_{TL}\frac{\delta^2 \ln \Xi_\Lambda^\star}{\delta z(\mathcal{E}_a)\delta z(\mathcal{E}_b)} \tag{38}$$

It can be represented by series of Mayer graphs Γ in terms of the filament density

https://doi.org/10.1017/S0252921100026312 Published online by Cambridge University Press

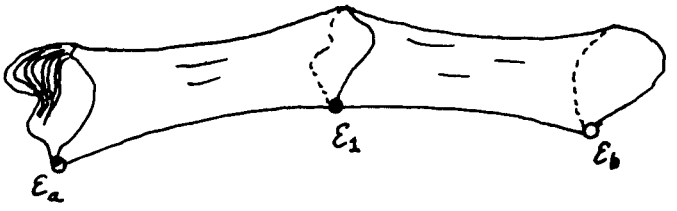

Fig. 1.7 A typical graph Γ which contributes to the Mayer-like density-expansion of $h(\mathcal{E}_a, \mathcal{E}_b)$. The closed filaments are drawn as in Figure 5, with the sole difference that the positions of the root filaments $\mathcal{E}_a$ and $\mathcal{E}_b$ are representated by white circles. The tubes connecting the filaments are the Mayer bonds $f(\mathcal{E}_a, \mathcal{E}_1)$ and $f(\mathcal{E}_1, \mathcal{E}_b)$.

$$\rho(\mathcal{E}) = z(\mathcal{E}) \lim_{TL} \frac{\delta \ln \Xi_\Lambda^\star}{\delta z(\mathcal{E})} \tag{39}$$

The Γ's are defined via the familiar topological prescriptions, where the usual points are now replaced by filaments. Each graph is built with the two root filaments $\mathcal{E}_a$ and $\mathcal{E}_b$ and n field filaments $\mathcal{E}_1,...,\mathcal{E}_n$ which are integrated over. Each field filament $\mathcal{E}_i$ has a statistical weight $\rho(\mathcal{E}_i)$. Two filaments are linked by at most one f-bond (33). Each Γ is connected and does not contain articulation filaments. A typical graph Γ is drawn in Figure 7 and its contribution reads

$$\int d\mathcal{E}_1 \rho(\mathcal{E}_1) f(\mathcal{E}_a, \mathcal{E}_1) f(\mathcal{E}_1, \mathcal{E}_b) \tag{40}$$

Note that the filament density $\rho(\mathcal{E}_1)$ cannot be factored outside the integral in (40) because it depends on the shape of the filament.

The contribution of each graph Γ is divergent because of the non-integrable 1/r-decay of the Mayer bond f associated to the Coulombic behaviour (31) of the potential v. For instance, the spatial integral over $\vec{r}_1$ involved in (40) is not convergent at large distances. The resummation procedure starts with the following decomposition

https://doi.org/10.1017/S0252921100026312 Published online by Cambridge University Press

$$f(\mathcal{E},\mathcal{E}') = f_C(|\vec{r}-\vec{r}'|) + \frac{1}{2}f_C^2(|\vec{r}-\vec{r}'|) + \int_0^1 ds[\lambda_\alpha \vec{\xi}(s).\vec{\nabla} + \lambda_{\alpha'}\vec{\xi}'(s).\vec{\nabla}']f_C(|\vec{r}-\vec{r}'|) + f_T(\mathcal{E},\mathcal{E}') \tag{41}$$

where f_c is the Coulomb shape-independent bond

$$f_C(|\vec{r}-\vec{r}'|) = -\beta e_\alpha e_{\alpha'} v_C(|\vec{r}-\vec{r}'|) \tag{42}$$

This decomposition defines in fact the truncated bond f_T. By construction f_T decays as $1/|\vec{r}-\vec{r}\,'|^3$ when $|\vec{r}-\vec{r}\,'|\to\infty$. Inserting (41) in each graph Γ, we obtain a new representation of $h(\mathcal{E}_a, \mathcal{E}_b)$ in terms of graphs $\tilde{\Gamma}$ built with bonds $\tilde{f}$ which maybe either f_c, $f_c^2/2$, $\lambda\vec{\xi}.\vec{\nabla}f_c$ or f_T.

Since f_T is almost integrable, the divergencies in the $\tilde{\Gamma}$-diagrams are induced by the other non-integrable bonds $\tilde{f}$. They are of the same type as those encountered in the purely classical case, so they can be eliminated via the same mathematical recipe (first introduced by Mayer (1950) and Salpeter (1957)), i.e., the resummation of all the convolution chains built with the Coulomb bond f_c. This procedure transforms the whole set of $\tilde{\Gamma}$-diagrams into a set of new graphs Π built with resummed bonds. For obtaining the graphs Π, one first distributes all the diagrams $\tilde{\Gamma}$ in resummation classes characterized by given chain-structures. For instance in Figures 8a, 8b and 8c we show three diagrams $\tilde{\Gamma}$ belonging to the same class. The summation of all the $\tilde{\Gamma}$-diagrams in a given class, then amounts to suppress all the intermediate filaments $\mathcal{C}$ in the Coulomb convolution chains, while the remaining filaments $\mathcal{P}$ are linked by resummed bonds F which reduce to the sums of these chains. The graph Π generated by the $\tilde{\Gamma}$-class illustrated in Figure 8, is drawn in Figure 9. The topological structure of the genuine graphs is conserved through the resummation process.

As a remarkable consequence of a factorization property of the symmetry counting factors, the resummed bonds F are generic in the sense that they do not depend on the global structure of the graphs Π. In fact, $F(\mathcal{P}_i,\mathcal{P}_j)$ only depends on the chain structures inserted between $\mathcal{P}_i$ and $\mathcal{P}_j$ in the genuine $\tilde{\Gamma}$-diagrams. Only four kinds of F-bonds appear. The single chains with ending bonds which are either f_c or $\lambda_i\vec{\xi}_i.\vec{\nabla}_i f_c$ ($\lambda_j\vec{\xi}_j.\vec{\nabla}_j f_c$), lead to three resummed bonds F_D, ($\lambda\vec{\xi}.\vec{\nabla}F_D$) and F_{dip}. All the other structures, involving several chains and/or the bonds f_T and $f_c^2/2$, give raise to the fourth bond F_R. All these cases are illustrated in Figures 8 and 9. The resummation procedure automatically excludes the convolutions $F_D * F_D$,

https://doi.org/10.1017/S0252921100026312 Published online by Cambridge University Press

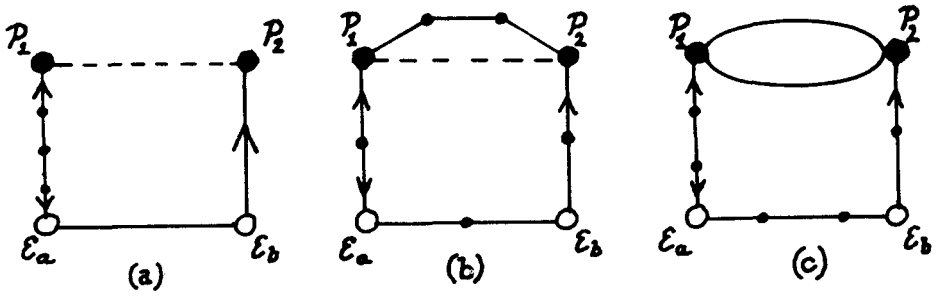

Fig. 1.8 a, 1.8b, 1.8c : Three $\tilde{\Gamma}$-diagrams which belong to the same resummation class. For clarity, the shapes of the filaments are not represented. The big black circles are filaments $\mathcal{P}$ which remain fixed through the resummation process. The small black circles are filaments $\mathcal{C}$ which are "eaten" by the resummation "machinery". Solid lines : bonds f_c ; lines with one arrow : bonds $\lambda\vec{\xi}.\vec{\nabla}f_c$ (the arrow indicates the point with respect to which acts the gradient) ; double solid lines : bonds $f_c^2/2$; dashed lines : bonds f_T.

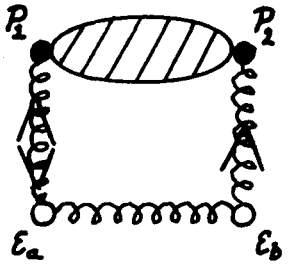

Fig. 1.9 The II-graph generated by the $\tilde{\Gamma}$-class illustrated in Figures 8a, 8b and 8c. Strings : bonds F_D ; strings with one arrow : bonds $\lambda\vec{\xi}.\vec{\nabla}F_D$; strings with two opposite arrows : bonds F_{dip} ; hatched bubbles : bonds F_R.

$\lambda_i\vec{\xi}_i.\vec{\nabla}_iF_D * F_D$, $F_D * \lambda_j\vec{\xi}_j.\vec{\nabla}_jF_D$ and $\lambda_i\vec{\xi}_i.\vec{\nabla}_iF_D * \lambda_j\vec{\xi}_j.\vec{\nabla}_jF_D$ between two filaments $(\mathcal{P}_i, \mathcal{P}_j)$ in any graph II.

The bonds F can be calculated explicitely in terms of the MB particle densities. Indeed, since the f_c-bonds are shape-independent, the functional

https://doi.org/10.1017/S0252921100026312 Published online by Cambridge University Press

integrations over the shapes of the intermediate filaments $\mathcal{C}$ in the chains lead to the replacement of each $\rho(\mathcal{E}) = \rho_\alpha(\vec{\xi})$ by the MB particle density

$$\rho_\alpha^{MB} = \int \mathcal{D}(\vec{\xi})\rho_\alpha(\vec{\xi}) \tag{43}$$

Thus the summation of all the convolution chains can be performed in terms of the familiar Debye potential $\phi_D(r) = \exp(-\kappa r)/r$ with $\kappa = (4\pi\beta\sum_\alpha e_\alpha^2 \rho_\alpha^{MB})^{1/2}$. In particular, one finds

$$F_D(\mathcal{P}_i, \mathcal{P}_j) = -\beta e_{\alpha_i} e_{\alpha_j} \phi_D(|\vec{r}_i - \vec{r}_j|) \tag{44}$$

We stress that , contrarily to F_D and $\lambda\vec{\xi}.\vec{\nabla}F_D$ which decay exponentially fast (like ϕ_D essentially), the bonds F_{dip} and F_R are found to decay algebraically as $1/r^3$ when $r \to \infty$. These behaviours are related to the efficiency of the screening of the multipole-like interactions, which appear in the expansion of the bare filament-filament potential (33) in powers of $\vec{\xi}$ and $\vec{\xi}'$. The charge-charge and dipole-charge interactions are perfectly screened via the usual classical process while the screening of the higher order multipole interactions is inhibited by quantum fluctuations. The above slow decays should ultimately pollute the correlations with algebraic tails, in accord with the absence of exponential clustering predicted by Brydges-Seiler (1986), Alastuey-Martin (1988-1989) and Cornu-Martin (1991). Although the screening mechanisms are less efficient than in the classical case, they do eliminate the long-range Coulomb divergencies, i.e., each graph II does converge, as expected.

The resummed diagrammatic expansion of the two-point correlations of S_{MB} is immediately obtained by inserting the previous II-representation of $h(\mathcal{E}_a, \mathcal{E}_b)$ in the identity

$$\rho_T^{MB}(\alpha_a\vec{r}_a; \alpha_b\vec{r}_b) = \int \mathcal{D}(\vec{\xi}_a)\mathcal{D}(\vec{\xi}_b)\rho(\mathcal{E}_a)\rho(\mathcal{E}_b)h(\mathcal{E}_a, \mathcal{E}_b) \tag{45}$$

In (45), each graph II is multiplied by $\rho(\mathcal{E}_a)\ \rho(\mathcal{E}_b)$ and integrated over the shapes $\vec{\xi}_a$ and $\vec{\xi}_b$ of the root filaments $\mathcal{E}_a$ and $\mathcal{E}_b$. Note that if we set $\hbar \to 0$, the bonds $\lambda\vec{\xi}.\vec{\nabla}F_D$ and F_{dip} disappear, while the bond F_R reduces to $(\exp(F_D) - 1 - F_D)$ and the statistical weights $\rho(\mathcal{E})$ are replaced by the particle densities. The so-called nodal expansion of the classical correlations first derived by Meeron (1958) is then recovered.

https://doi.org/10.1017/S0252921100026312 Published online by Cambridge University Press

3.4.2 *The MB thermodynamic functions*

For evaluating the density expansions of the MB thermodynamic functions, it is convenient to start from the identity

$$\frac{\beta F^{MB}}{\Lambda} = \frac{\beta F_{id}^{MB}}{\Lambda} + \frac{\beta}{2}\sum_{\alpha,\beta}\int_0^1 dg \int d\vec{r}\rho_{T,g}^{MB}(\alpha\vec{0},\beta\vec{r})e_\alpha e_\beta v_C(r) \qquad (46)$$

which expresses the free-energy per unit of volume in terms of the two-point correlations. In (46), $\rho_{T,g}^{MB}$ is calculated for a fictitious system $\mathcal{S}_g$ where all the interactions are multiplied by the dimensionless coupling parameter g. Moreover the temperature and the MB particle densities of $\mathcal{S}_g$ are identical to those of $\mathcal{S}$. The insertion of the II-representation of $\rho_{T,g}^{MB}$ in (46) provides a diagrammatic expansion of the free-energy.

At this level, the II-series for $(\beta F^{MB}/\Lambda)$ do not constitute an explicit expansion with respect to the particle densities, because of the presence of the shape-dependent statistical weights $\rho_g(\mathcal{E})$. In fact, the functional $\rho_g(\mathcal{E})$ can be itself expanded in powers of the ρ_α^{MB}'s as follows. One starts from the familiar Mayer expansion of $\rho_g(\mathcal{E})$ in terms of the fugacities $z(\mathcal{E}) = z_\alpha^*$. The corresponding set of divergent Mayer graphs G is then transformed into a set of convergent graphs P via a resummation process similar to the one described in Section 4.1. Now there appear five resummed bonds which can be expressed in terms of functions entirely scaled by $\kappa_{D,z} = (4\pi\beta\sum_\alpha e_\alpha^2 z_\alpha)^{1/2}$ and of f_T scaled by the Landau and de Broglie lengths (these lengths depend only on the temperature). A scaling analysis with respect to $\kappa_{D,z}$ of the spatial integrals in the graphs P allows to express $\rho_g(\mathcal{E})$ as a double integer series in $z^{*1/2}$ and lnz^*. The half-integer powers come from $\kappa_{D,z} \sim z^{*1/2}$ while the logarithms arise from the $1/r^3$-tail in f_T. Eventually, the fugacities are eliminated in favor of the particle densities by using (43), and $\rho_g(\mathcal{E})$ is rewritten as a double integer series in $(\rho^{MB})^{1/2}$ and $\ln\rho^{MB}$, the first terms of which read

$$\begin{aligned}\rho_g(\mathcal{E}) =& \rho_\alpha^{MB} + \sum_\gamma \rho_\alpha^{MB}\rho_\gamma^{MB}\int d\vec{r}\int \mathcal{D}(\vec{\xi}_1) \\ &\left[\exp\left(-\beta g e_\alpha e_\gamma \int_0^1 ds v_C(|\vec{r}+\lambda_\gamma\vec{\xi}_1(s)-\lambda_\alpha\vec{\xi}(s)|)\right)\right. \\ &\left. - \int \mathcal{D}(\vec{\xi}\prime)\exp\left(-\beta e_\alpha e_\gamma \int_0^1 ds v_C(|\vec{r}+\lambda_\gamma\vec{\xi}_1(s)-\lambda_\alpha\vec{\xi}\prime(s)|)\right)\right] \\ &+ O(\rho^{5/2})\end{aligned} \qquad (47$$

After the replacement of the statistical weights $\rho_g(\mathcal{E})$ by their particle-

https://doi.org/10.1017/S0252921100026312 Published online by Cambridge University Press

densities expansions, it remains to determine the density dependence of the spatial integrals in the Π-graphs. This analysis is carried out via a scaling method similar to the one used for the P-graphs with κ_D in place of $\kappa_{D,z}$. Indeed, all the resummed bonds F can be expressed in terms of κ_D-scaled functions and f_T. The final form of the density expansion of $(\beta F^{MB}/\Lambda)$ is a double integer series in $(\rho^{MB})^{1/2}$ and $ln\rho^{MB}$. The corresponding expansion of the pressure βP^{MB} derived from the identity

$$\beta P^{MB} = \sum_\alpha \rho_\alpha^{MB} \frac{\partial}{\partial \rho_\alpha^{MB}} \Big(\lim_{TL} \Big[\frac{\beta F_\Lambda^{MB}}{\Lambda} \Big] \Big) |_\beta - \lim_{TL} \Big[\frac{\beta F_\Lambda^{MB}}{\Lambda} \Big] \tag{48}$$

has the same structure.

We stress that the macroscopic instability of $\mathcal{S}^{MB}$ does not cause any divergency in the virial coefficients of the above series. However, it should prevent their convergence.

3.4.3 *Exchange contributions*

The exchange effects are taken into account by inserting the Slater expansion (35) of Ξ_Λ in the grand-canonical expression (3) of βP. This gives

$$\beta P = \beta P^{MB} + \sum_{n=2}^{\infty} E_n \tag{49}$$

where E_n is the contribution of n exchanged particles. According to the impurities point of view, E_n may be expressed in terms of the density $\rho(\mathcal{E}_a|\mathcal{F}_{kl})$ of $\mathcal{S}^*$ in presence of n opened filaments $\mathcal{F}_{kl}$. For instance, E_2 reads

$$\begin{aligned} E_2 = & -\frac{1}{2} \sum_\alpha (-1)^{2\sigma_\alpha+1} (2\sigma_\alpha+1) \frac{z_\alpha^2}{(2\pi\lambda_\alpha^2)^3} \int_\Lambda d\vec{r}_{12} \int \mathcal{D}(\vec{\xi}_1)\mathcal{D}(\vec{\xi}_2) \\ & \times \exp\Big[\frac{-r_{12}^2}{\lambda_\alpha^2} - \beta v(\mathcal{F}_{12}^\alpha, \mathcal{F}_{21}^\alpha) \Big] \\ & \times \exp\Big[-\beta \int_0^1 dg \int d\mathcal{E}_a \rho(\mathcal{E}_a|g; \mathcal{F}_{12}^\alpha, \mathcal{F}_{21}^\alpha) \Big(v(\mathcal{E}_a, \mathcal{F}_{12}^\alpha) + v(\mathcal{E}_a, \mathcal{F}_{21}^\alpha) \Big) \Big] \end{aligned} \tag{50}$$

In (50), the first exponential represents the exchange contribution in the vacuum while the second one describes the many-body effects on the two-particle exchange. The structure of all the other E_n's is similar to the one displayed in (50).

The diagrammatical method exposed in Section 4.1 can be extended to

https://doi.org/10.1017/S0252921100026312 Published online by Cambridge University Press

the inhomogeneous system $\mathcal{S}^*$ in presence of the $\mathcal{F}$'s. This provides a representation of $\rho\,(\mathcal{E}_a|\mathcal{F}_{kl})$ in terms of graphs made of the n opened filaments $\mathcal{F}_{kl}$ and closed filaments. The statistical weight of a closed filament is the density $\rho(\mathcal{E})$ of the homogeneous system. Two closed filaments are linked by at most one resummed bond F. A closed filament $\mathcal{E}$ and an opened filament $\mathcal{F}$ are linked by at most one "external" Mayer bond $(\exp\,[-\beta v(\mathcal{E},\mathcal{F})]-1)$.

The density expansion of E_n follows from use of the previous diagrammatic representation of $\rho(\mathcal{E}_a|\mathcal{F}_{kl})$. The integrals over the positions of the opened and closed filaments can be evaluated via a scaling analysis with respect to κ_D. The resulting expression for E_n takes the general form z^n multiplied by a double integer series in $(\rho^{MB})^{1/2}$ and $ln\rho^{MB}$.

3.4.4 *General structure of the density expansions*

The present method gives access first to the pressure. Use of the expansions of βP^{MB} and E_n in (52), allows to rewrite βP as a triple integer series in z, $(\rho^{MB})^{1/2}$ and $\ln\rho^{MB}$. The fugacities and MB densities are then eliminated in favor of the real densities ρ_α by combining the identities $\rho_\alpha^{MB} = z_\alpha\partial(\beta P^{MB})/\partial z_\alpha$ and $\rho_\alpha = z_\alpha\partial(\beta P)\,/\,\partial z_\alpha$ (ρ_α^{MB} differs from ρ_α at given fugacities). The resulting virial expansion of the pressure is a double integer series in $\rho^{1/2}$ and $ln\rho$. The density expansions of the other thermodynamic functions, obtained via the usual identities, have the same structure.

According to the above scaling analysis, the contributions of a fully resummed graph of the II-type to a given virial coefficient, reduce to subgraphs built with bonds f_T, F_D, f_c, $\lambda\vec{\xi}.\vec{\nabla}F_D$, $\lambda\vec{\xi}.\vec{\nabla}f_c$. The physical nature of these contributions can then be identified by inspection of the bonds and filaments which appear in the subgraphs according to the correspondance rules,

- long-range classical interactions : bonds f_c and F_D
- quantum diffraction : bonds $\lambda\vec{\xi}.\vec{\nabla}f_c$ and $\lambda\vec{\xi}.\vec{\nabla}F_D$
- bound and scattering states : bonds f_T
- exchange : opened filaments

In general, all these physical effects are coupled at high orders in ρ. We stress that, in the present formalism, all the corresponding contributions are treated simultaneously in a systematic and coherent way.

Of course, the exact density expansions can be also derived in the framework of the formalisms described in Section 2. However, the FK diagrammatic method is well-suited for this purpose. In particular, all the long-

https://doi.org/10.1017/S0252921100026312 Published online by Cambridge University Press

range Coulomb divergencies are automatically eliminated at any order in the density via the introduction of the generic resummed bonds F. In the effective-potential method, it remains to treat the long-range part of the many-body effective interactions in a systematic way. Furthermore, the density is the natural expansion-parameter in the FK diagrammatics. Indeed only a finite number of graphs Π contributes to a given virial coefficient (roughly speaking the order in the density of Π increases with the number of filaments and the number of bonds). On the contrary, the calculation of such a coefficient from many-body perturbation requires the collection of infinite sets of Feynman graphs with Ladder structures. Moreover, in this approach, the elimination of the fugacities in favor of the densities is more cumbersome than in the FK method where part of this transformation is automatically done.

Although the FK representation is quite efficient for performing infinite resummations at a formal level, one has to keep in mind that, for practical calculations, the difficulty relies in the functional integration over the shapes of the filaments. The purely diffraction contributions, which only involve moments of the Gaussian measure $\mathcal{D}(\vec{\xi})$, are evaluated from the covariance (28) by using Wick's theorem. The contributions of bound and scattering states, which involve one or more bonds f_T, cannot be so easily computed in the space of filaments. In fact, it is more convenient to express them in terms of matrix elements of exp $(-\beta H_N)$ by applying backwards the FK formula (26). The corresponding explicit calculations are then limited by the absence of exact solutions for the N-body quantum-mechanical problem, as soon as N is larger than two. Beside the complexity of the graphs, this problem intrinsic to quantum mechanics and which appear in any formalism, prevent a detailed knowledge of the virial coefficients at orders higher than $\rho^{5/2}$.

3.5 Low-Density Equations of State

3.5.1 *the exact EOS at the order* $\rho^{5/2}$

The truncation of the above virial expansion of the pressure at the order

https://doi.org/10.1017/S0252921100026312 Published online by Cambridge University Press

$\rho^{5/2}$ gives (Alastuey and Perez (1992))

$$\begin{aligned}
\beta P = & \sum_\alpha \rho_\alpha - \frac{\kappa_D^3}{24\pi} \\
& + \frac{\pi}{6}(\ln 2 - 1) \sum_{\alpha,\beta} \beta^3 e_\alpha^3 e_\beta^3 \rho_\alpha \rho_\beta \\
& - \frac{\pi}{\sqrt{2}} \sum_{\alpha,\beta} \rho_\alpha \rho_\beta \lambda_{\alpha\beta}^3 Q(x_{\alpha\beta}) - \frac{\pi}{3}\beta^3 \sum_{\alpha,\beta} \rho_\alpha \rho_\beta e_\alpha^3 e_\beta^3 \ln(\kappa\lambda_{\alpha\beta}) \\
& + \frac{\pi}{\sqrt{2}} \sum_\alpha \frac{(-1)^{2\sigma_\alpha+1}}{(2\sigma_\alpha+1)} \lambda_{\alpha\alpha}^3 \rho_\alpha^2 E(x_{\alpha\alpha}) \\
& - \frac{3\pi}{2\sqrt{2}}\beta \sum_{\alpha,\beta} e_\alpha e_\beta \kappa \rho_\alpha \rho_\beta \lambda_{\alpha\beta}^3 Q(x_{\alpha\beta}) \\
& - \frac{\pi}{2}\beta^4 \sum_{\alpha,\beta} \rho_\alpha \rho_\beta e_\alpha^4 e_\beta^4 \kappa \ln(\kappa\lambda_{\alpha\beta}) \\
& + \frac{3\pi}{2\sqrt{2}}\beta \sum_\alpha \frac{(-1)^{2\sigma_\alpha+1}}{(2\sigma_\alpha+1)} \lambda_{\alpha\alpha}^3 \rho_\alpha^2 e_\alpha^2 \kappa E(x_{\alpha\alpha}) \\
& + \frac{1}{16} \sum_\alpha \frac{\beta^2\hbar^2 e_\alpha^2}{m_\alpha} \kappa^3 \rho_\alpha + \pi(\frac{1}{3} - \frac{3}{4}\ln 2 + \frac{1}{2}\ln 3) \sum_{\alpha,\beta} \beta^4 e_\alpha^4 e_\beta^4 \kappa \rho_\alpha \rho_\beta \\
& + C_1 \sum_{\alpha,\beta,\gamma} \beta^5 e_\alpha^3 e_\beta^4 e_\gamma^3 \kappa^{-1} \rho_\alpha \rho_\beta \rho_\gamma \\
& + C_2 \sum_{\alpha,\beta,\gamma,\delta} \beta^6 e_\alpha^3 e_\beta^3 e_\gamma^3 e_\delta^3 \kappa^{-3} \rho_\alpha \rho_\beta \rho_\gamma \rho_\delta
\end{aligned} \tag{51}$$

with $\kappa_D = (4\pi\beta \sum_\alpha e_\alpha^2 \rho_\alpha)^{1/2}$, $l_{\alpha\beta} = \beta e_\alpha e_\beta$, $m_{\alpha\beta} = m_\alpha m_\beta/(m_\alpha+m_\beta)$, $\lambda_{\alpha\beta} = (\beta\hbar^2/m_{\alpha\beta})^{1/2}$, $C_1 = 15.205 \pm .001$, $C_2 = -14.733 \pm .001$ and Euler-Mascheroni's constant $C = .577216\ldots$ Moreover, $Q(-\sqrt{2}l_{\alpha\beta}/\lambda_{\alpha\beta})$ is the so-called quantum second-virial coefficient first introduced by Ebeling

$$\begin{aligned}
Q(-\sqrt{2}\frac{l_{\alpha\beta}}{\lambda_{\alpha\beta}}) = & \frac{1}{(\sqrt{2}\pi\lambda_{\alpha\beta}^3)} \lim_{R\to\infty} \Big\{ \int_{r<R} d\vec{r} \Big[(2\pi\lambda_{\alpha\beta}^2)^{3/2} < \vec{r}|e^{-\beta h_{\alpha\beta}}|\vec{r} > \\
& - 1 + \frac{\beta e_\alpha e_\beta}{r} - \frac{\beta^2 e_\alpha^2 e_\beta^2}{2r^2} \Big] + \frac{2\pi}{3}\beta^3 e_\alpha^3 e_\beta^3 [\ln(\frac{3\sqrt{2}R}{\lambda_{\alpha\beta}}) + C] \Big\}
\end{aligned} \tag{52}$$

while $E(-\sqrt{2}l_{\alpha\alpha}/\lambda_{\alpha\alpha})$ is the exchange integral,

https://doi.org/10.1017/S0252921100026312 Published online by Cambridge University Press

$$E(-\sqrt{2}\frac{l_{\alpha\alpha}}{\lambda_{\alpha\alpha}}) = (2\sqrt{\pi}) \int d\vec{r} < -\vec{r}|e^{-\beta h_{\alpha\alpha}}|\vec{r} > \tag{53}$$

In (52) and (53), $h_{\alpha\beta}$ is the one-body Hamiltonian of the relative particle with mass $m_{\alpha\beta}$ submitted to the Coulomb potential $e_\alpha e_\beta / r$. The functions Q and E only depend on the temperature via the single dimensionless parameter $(-\sqrt{2}l/\lambda)$. All the physical effects mentioned is Subsection 4.4 give contributions to (51), the structures of which require the following comments.

First, the classical contributions of the long-range part of the interactions are polynomials in the inverse temperature, the charges and the densities, which do not involve Planck's constant. The involved coefficients are evaluated analytically or, like C_1 and C_2, by numerical computations of dimensionless integrals. The lowest-order contribution is nothing but the familiar Debye-Hückel term in $\rho^{3/2}$, and constitutes the leading correction to the MB ideal pressure in (51). By specifying (51) to the case of the classical OCP, it can be checked that the classical terms found here, up to the order $\rho^{5/2}$, do coincide with those calculated by Cohen and Murphy (1971), as it should be.

The contribution of quantum diffraction at large distances appears only at the order $\rho^{5/2}$ and reduces to

$$\frac{1}{16} \sum_\alpha \frac{\beta^2 \hbar^2 e_\alpha^2}{m_\alpha} \kappa^3 \rho_\alpha \tag{54}$$

The occurence of this term shows that the long-range part of the interactions cannot be entirely treated at a classical level. This diffraction term is missing in the expressions obtained by the effective-potential method. In this formalism, it arises from the three-body interactions $u^{(3)}$ which are long-ranged. Indeed, for large-triangular configurations, $u_{123}^{(3)}$ typically behaves as $(\beta^3 \hbar^2 e_1^2 e_2 e_3 / (12 m_1)) \vec{\nabla}_1 v_c(r_{12}) . \vec{\nabla}_1 v_c(r_{13})$ (apart from a sum over the permutations of 1, 2, 3). These slow $1/r^2$-decays lead to screened contributions which are of order $\rho^{5/2}$ instead of ρ^3 (a similar mechanism makes the Debye correction be of order $\rho^{3/2}$ instead of ρ^2). The diffraction correction (54) is merely proportional to $\hbar^2$, because it arises from large distances where the quantum effects can be treated perturbatively "*à* la Wigner-Kirkwood". By the way, the presence of this term is crucial for recovering from (51) the well-known $\hbar^2$-correction (Hansen and Pollock (1973))

https://doi.org/10.1017/S0252921100026312 Published online by Cambridge University Press

$$\frac{\pi\beta^2 e^2 \rho^2 \hbar^2}{6m} \tag{55}$$

to the classical pressure of the OCP calculated by the WK method. In fact, the sole contributions to (55) do arise only from the ρ^2-term in (51), while (54) exactly cancels the $\hbar^2$-term which comes from $\rho^2 \kappa_D Q$.

The term $\rho_\alpha \rho_\beta \lambda_{\alpha\beta}^3 Q(-\sqrt{2} l_{\alpha\beta}/\lambda_{\alpha\beta})$ is the total contribution from both bound and scattering states of two charges e_α and e_β. The truncation of $< \vec{r}\,|\exp(-\beta h_{\alpha\beta})|\,\vec{r}\,>$ in the integral (52) defining Q ensures that this contribution is finite. This regularization in not an arbitrary mathematical artefact. It is directly related to the truncated stucture of the bond f_T, and reflects the screening of the Coulomb interaction at large distances. For opposite charges such that $e_\alpha e_\beta < 0$, one may extract from Q a contribution of the bound states which reduces to the familiar Planck-Brillouin-Larkin (PBL) sum

$$\sum_{n=1}^{\infty} n^2 \left[\exp(-\beta\epsilon_n^{\alpha\beta}) - 1 + \beta\epsilon_n^{\alpha\beta}\right] \tag{56}$$

where $\epsilon_n^{\alpha\beta} = -e_\alpha^2 e_\beta^2 m_{\alpha\beta}/(2\hbar^2 n^2)$ are the energy levels of the hydrogenoid atom with Hamiltonian $h_{\alpha\beta}$. However, other definitions of the bound states contributions can be introduced from (52) by using the basic properties of the trace. For instance, as shown by Bollé (1987), there exists an infinite set of arbitrary decompositions in terms of bound and scattering contributions of the PBL sum itself. So, as far as thermodynamic quantities are concerned, only the total contribution of both bound and scattering states is an unambiguous quantity. The $\rho^{5/2}$-contribution from bound and scattering states merely reduces to its ρ^2 counterpart multiplied by $\beta e_\alpha e_\beta \kappa_D$. This multiplicative factor arises from many-body effects which induce a constant shift $-e_\alpha e_\beta \kappa_D$ on the energy levels of the two-particles states.

The contribution $\rho_\alpha^2 E(-\sqrt{2} l_{\alpha\alpha}/\lambda_{\alpha\alpha})$ arises from the exchange of two charges e_α in the vacuum. It is finite, independently of any screening effect, because the off-diagonal matrix elements $< -\vec{r}\,|\exp(-\beta h_{\alpha\alpha})|\,\vec{r}\,>$ are short-ranged. The magnitude of this contribution is smaller than the one relative to free particles because the repulsive potential e_α^2/r inhibits the exchange. Similarly to what happens for the contributions of bound and scattering states, at the order $\rho^{5/2}$, the many-body effects on the two-particles exchange amount to lower the repulsive barrier e_α^2/r by the constant $-e_\alpha^2 \kappa_D$.

https://doi.org/10.1017/S0252921100026312 Published online by Cambridge University Press

Eventually, the high-temperature series can be recovered from (51) by expanding the virial-coefficients in powers of β. Since l/λ is proportional to $\beta^{1/2}$, the β-expansions of $Q\ (-\sqrt{2}l/\lambda)$ and $E\ (-\sqrt{2}l/\lambda)$ coincide with their Taylor series in powers of l/λ. In agreement with DeWitt's observations, such series do involve singular powers of $\hbar$ because l/λ is also proportional to $1/\hbar$. In fact, the expression (23) up to the order $\beta^{5/2}$ is exactly recovered by inserting the β-expansions of Q and E in (51). The calculation of the higher order terms from the virial expansion requires a suitable reorganization of the density series, similar to the one relative to the e^2-series evocated in Section 2.2.

3.5.2 *Application to the Sun*

For practical applications, the range of validity of the truncated EOS (51) is determined by the conditions $l < a$ and $\lambda < a$ (with $a \sim \rho^{-1/3}$), which mean respectively weak coupling and weak degeneracy. It turns out that these conditions are met in the inner regions of the Sun which can be viewed, in a first approximation, as a three-component plasma made of electrons, protons and Helium nuclei. Perez (private communication) has evaluated the various physical corrections appearing in (51) within a typical temperature- and density-profile. Moreover, he used representations of Q (Kraeft et al (1986)) and E (Jancovici (1978)) which allow simple and accurate numerical computations. His results are sketched in Table 1. As expected, the inner regions almost behave as an ideal MB gas, since the relative magnitudes of the above corrections do not exceed a few percent. In the core, the correction to the ideal MB pressure is positive and mainly due to the electronic exchange. In the outer layers, this correction becomes negative because the classical Debye term then dominates. In the intermediate regions, the partial cancellation between the exchange and Debye terms increases the relative importance of the other contributions in (51), in particular those taking into account the recombinations between one nuclei and one electron in hydrogen atoms and He^+ ions.

The previous results illustrate the usefulness of the truncated EOS (51) for helioseismology. The actual observations lead to very accurate determinations of the speed of the sound and of adiabatic coefficients. For a proper interpretation of these data, one needs a reliable theoretical description of the small deviations from the ideal behaviour. The EOS (51) fullfills this requirement since it comes out from an exact expansion. Furthermore, its analytical character allows simple and consistent calculations of any thermodynamic coefficient via partial differentiations with respect to the density

Table 1.1. *Relative deviations from the MB ideal pressure for the inner regions of the Sun, calculated from the truncated EOS (51). R represents the distance to the center. The magnitudes of all the physical corrections arising in (51) are also indicated*

R	$\log\rho$	$\log T$	$\beta P/\rho - 1$	Class. Int.	Bound/ Scatt.St.	Exch.	Diff.
$[10^6]$ km	g/cc	(K)	$[10^{-2}]$	$[10^{-2}]$	$[10^{-2}]$	$[10^{-2}]$	$[10^{-2}]$
0.62	−2.2	5.82	−0.698	−0.710	0.006	0.005	0.000
0.15	1.5	6.95	0.110	−1.000	0.089	1.006	0.014
0.00	2.2	7.19	1.446	−0.971	0.101	2.294	0.022

or the temperature. This EOS should be quite efficient for describing the regions close to the core, where all the chemical species are almost fully ionized (the inclusion of the contributions of heavier nuclei, like F_e^{26+}, is straightforward). Near the surface, the validity of the $\rho^{5/2}$-truncated EOS is limited by the presence of atoms (like He) and ions which result from recombinations between one nuclei and two or more electrons. In the virial expansions, the contributions of these entities enter in terms of order ρ^3 (at least) which are not included in (51).

Acknowledgment

I am indebted to Marie-Pierre Fuchs for typing this manuscript, and to Asher Perez for communicating unpublished data.

References

Abe R., *Progr. Theor. Phys.* **22**, 213, (1959)
Alastuey A., Cornu F. and Perez A., *to be published in Phys. Rev. E*, (1994)
Alastuey A. and Martin Ph. A., *Phys. Rev.* **A 40**, 6485, (1989)
Alastuey A. and Perez A., *Europhys. Lett.* **20**, 19, (1992)
Bollé D., *Phys. Rev.* **A 36**, 3259, (1987)
Brydges D. and Seiler E., *J. Stat. Phys.* **42**, 405, (1986)
Chandler D., *"Studies in Statistical Mechanics"*, edited by E. W. Montroll and J. L. Lebowitz (North Holland, Amsterdam, 1981)
Cohen E. G. D. and Murphy T. J., *Phys. Fluids* **12**, 1404, (1969)
Cornu F. and Martin Ph. A., *Phys. Rev.* **A 44**, 4893, (1991)
De Witt H. E., *J. Math. Phys.* **3**, 1216, (1962)
De Witt H. E., *J. Math. Phys.* **7**, 616, (1966)
Dyson F. J. and Lenard A., *J. Math. Phys.* **8**, 423, (1967)
Ebeling W., *Ann. Phys. (Leipzig)* **19**, 104, (1967)
Fetter A. and Walecka J. D., *"Quantum Theory of Many-Particle Systems"* (Mc Graw-Hill, New York, 1971)

Feynman R. P. and Hibbs A. R., *"Quantum Mechanics and Path Integrals"* (Mc Graw-Hill, New York, 1965)
Gell-Mann M. and Brueckner K. A., *Phys. Rev.* **106**, 364, (1957)
Ginibre J., *"Statistical Mechanics and Quantum Field Theory "* (Les Houches Lectures, ed. by C. De Witt and R. Stora (Gordon and Breach, New York, 1971)
Jancovici B., *Physica* **91 A**, 152, (1978)
Kraeft W. D., Kremp D., Ebeling W. and Röpke G., *"Quantum Statistics of Charged Particle Systems"* (Plenum Press, New York, 1986)
Lenard A. and Dyson F. J., *J. Math. Phys.* **9**, 698, (1968)
Lieb E. H., *Rev. Mod. Phys.* **48**, 553, (1976)
Lieb E. H. and Lebowitz J. L.,*Adv. Math.* **9**, 316, (1972)
Mayer J. E., *J. Chem. Phys.* **18**, 1426, (1950)
Meeron E., *J. Chem Phys.* **28**, 630, (1958)
Montroll E. W. and Ward J. C., *Phys. Fluids* **1**, 55, (1958)
Morita T., *Prog. Theor. Phys. (Japan)* **22**, 757, (1959)
Pollock E. L. and Hansen J. P., *Phys. Rev.* **A 8**, 3110, (1973)
Rogers F. J., *Phys. Rev.* **A10**, 2441, (1974)
Salpeter E. E., *Ann. Phys.(New York)* **5**, 183, (1958)
Simon B., *"Functional Integration and Quantum Physics"* (Academic, New York, 1979)